

DMD #14241

INTERACTION OF POSITIONAL ISOMERS OF QUERCETIN GLUCURONIDES WITH  
THE TRANSPORTER ABCC2 (cMOAT, MRP2)

Gary Williamson, Isabelle Aeberli, Laurence Miguet, Ziding Zhang, M.-Belen Sanchez,  
Vanessa Crespy, Denis Barron, Paul Needs, Paul A. Kroon, H. Glavinas, Peter Krajcsi and  
Martin Grigorov

Nestlé Research Center, Lausanne, Switzerland (G.W., I.A., L.M., M-B.S., V.C., D.B., M.G.);  
Institute of Food Research, Norwich, UK (P.N., P.A.K.); Solvo Biotechnology, Hungary  
(H.G., P.K.); Rational Drug Design Laboratories, CRC, Budapest, Hungary (P.K.).

DMD #14241

Running title: Interaction of quercetin glucuronides with ABCC2

Address correspondence to: Gary Williamson, Nestlé Research Center, Vers Chez Les Blanc,  
1000 Lausanne 26, Switzerland, Tel. +41217858546; Fax. +41217858544;

E-mail: [gary.williamson@rdls.nestle.com](mailto:gary.williamson@rdls.nestle.com)

Number of pages: 15

Number of tables: 2

Number of figures: 4

Number of references: 40

Abstract: 221 words

Introduction: 541 words

Discussion: 693 words

Abbreviations: ABC, ATP-binding cassette; NBD, nucleotide-binding domain; TMD, trans-  
membrane domain; UGT, UDP-glucuronosyl transferase.

DMD #14241

## ABSTRACT

The exporter ABCC2 (cMOAT, MRP2) is a membrane bound protein on the apical side of enterocytes and hepatic biliary vessels that transports leukotriene C<sub>4</sub>, glutathione, some conjugated bile salts, drugs, xenobiotics and phytonutrients. The latter class includes quercetin, a bioactive flavonoid found in foods such as onions, apples, tea and wine. There is no available 3D structure of ABCC2. We have predicted the 3D structure by *in silico* modeling, showing that MK571 binds most tightly to the putative binding site, and then tested the computational prediction experimentally by measuring interaction with all quercetin mono-glucuronides occurring *in vivo* (quercetin substituted with glucuronic acid at the 3, 3', 4' and 7 hydroxyl groups). The 4'-*O*- $\beta$ -D-glucuronide is predicted *in silico* to interact most strongly, and the 3-*O*- $\beta$ -D-glucuronide most weakly, and this is supported experimentally using binding and competition assays on ABCC2 over-expressing baculovirus-infected Sf9 cells. To test the transport *in situ*, we examined the effect of two ABCC2 inhibitors, MK571 and cyclosporin A, on the transport into the media of quercetin glucuronides produced intracellularly by Caco2 cells. The inhibitors reduced the amount of all quercetin glucuronides in the media. The results show that the molecular model of ABCC2 agrees well with experimentally determined ABCC2-ligand interactions, and importantly that the interaction of ABCC2 with quercetin glucuronides is dependent on the position and nature of substitution.

DMD #14241

ABCC2 (cMOAT, MRP2) is a member of the family of ATP binding cassette (ABC) transporters. Lack of ABCC2 expression in humans leads to the Dubin-Johnson syndrome, an autosomal dominant hereditary disease (Konig et al., 1999). This manifests itself by chronic hyperbilirubinemia due to reduced biliary secretion of bilirubin conjugates (Payen et al., 2002). ABCC2 is a trans-membrane protein that uses the energy of ATP hydrolysis to translocate its substrates across biological membranes, and transports a wide variety of compounds, including various endobiotics and xenobiotics. Recent studies suggest that ABCC2 influences oral bioavailability (Dietrich et al., 2003) and its inhibition decreases the elimination of xenobiotics. It is structurally closely related to ABCC1 (MRP1) and the substrate selectivities of ABCC1 and ABCC2 overlap (Gerk and Vore, 2002) to a large extent.

The 1545-amino acid human ABCC2 contains two Nucleotide-Binding Domains (NBDs) and up to 17 trans-membrane helices distributed within three trans-membrane Domains (TMD) -1, -2 and -3. Classified into the same MRP family, the human ABCC1 and human ABCC2 share 48 % sequence identity as well as a similar membrane topology, implying structural and functional similarity. It has been shown that the amino terminal TMD-1 of ABCC1 is not essential for substrate transport. Experimental efforts to characterize the substrate binding/transport have therefore been focused on trans-membrane segments TM6 to TM17 of TMD-2 (TM6 to TM11) and TMD-3 (TM12 to TM17). To date, high-resolution 3D structures for ABCC1 and ABCC2 are still not available. The 3D structures for TMD-2 and -3 of ABCC1 have been obtained by homology modeling (Campbell et al., 2004). As revealed in the predicted 3D model, TMD-2 and -3 form a channel, which allows for the transportation of ABCC1 substrates. Together with biochemical studies, the 3D structural model for ABCC1 has provided further insight on the transport mechanisms (Campbell et al., 2004).

DMD #14241

Quercetin is an anticarcinogenic flavonoid which affects phase II enzyme-catalyzed detoxification, phosphorylation and cell signaling (Uda et al., 1997; Nagasaka and Nakamura, 1998; Spencer et al., 2003). During metabolism, it is conjugated with glucuronide, methyl and sulfate groups by the liver and small intestine (Gee et al., 2000; Day et al., 2001). Quercetin has five hydroxyl groups, and cellular glucuronidation of four of these (3, 3', 4' and 7 positions) has been reported. A proportion of quercetin which is taken up by the enterocyte is effluxed back to the intestinal lumen in humans (Petri et al., 2003) and rats (Crespy et al., 1999). Glucuronide conjugation at the 3 and 7 positions reduces dramatically the inhibition of xanthine oxidase and lipoxygenase (Day et al., 2000), whereas glucuronide conjugation at the 3' and 4' positions reduces the ability to prolong the lag time of human LDL oxidation in vitro (Janisch et al., 2004). One of the factors limiting quercetin absorption could be the interaction of its glucuronides with pumps such as ABCC2, limiting the absorption by effluxing the conjugates back into the intestinal lumen or into the bile (Petri et al., 2003). MK571 has been used extensively as an inhibitor of ABCC2 e.g. (Pulaski et al., 1996), and cyclosporin is also an inhibitor (Wortelboer et al., 2003). We used a combination of quercetin conjugates and inhibitors to test interaction with ABCC2 and to assess the predictive power of an *in silico* generated 3D model of ABCC2.

DMD #14241

## Materials and methods

*Materials*- Tamarixetin (4'-methylquercetin) and isorhamnetin (3'-methylquercetin) were purchased from Extrasynthese, Genay, France (both >99% pure). The ABCC2-Inhibitor MK571 and cyclosporin A were from Alexis Biochemicals, Switzerland. Synthesis of conjugates enzymatically was as previously described (Morand et al., 1998; Day et al., 2000). Quercetin-7-*O*- $\beta$ -D-glucuronide, quercetin-3-*O*- $\beta$ -D-glucuronide, quercetin-3'-*O*- $\beta$ -D-glucuronide and quercetin-4'-*O*- $\beta$ -D-glucuronide were chemically synthesized and characterized extensively as previously described (O'Leary et al., 2001; Pascual-Teresa et al., 2004) (Needs and Kroon, unpublished results).

*HPLC* - HPLC was performed using a Macherey-Nagel 100-5 C<sub>18</sub> 250 mm x 3 mm column and a gradient of 15% acetonitrile + 0.5% H<sub>3</sub>PO<sub>4</sub> + 84.5% water to 40% acetonitrile + 0.5% H<sub>3</sub>PO<sub>4</sub> + 59.5% water over 15 min at 0.4 ml/min, with detection at 370 nm. Quercetin and conjugates were analyzed essentially as previously described (Day et al., 2001; Crespy et al., 2004).

*Homology modeling for TMD-2 and -3 in ABCC2* - The fold identification for human ABCC2 (Swissprot entry: Q92887) was performed via several fold recognition servers (FFAS (Jaroszewski et al., 1998), SAMT99 (Karplus et al., 1998), Fugue (Shi et al., 2001)). Although no structural templates for TMD-1 were identified, the structural templates for TMD-2, -3 and two of the NBDs were confidently assigned. In our current investigation, we only focused on the structural modeling of TMD-2 and -3. All three of the fold recognition methods confidently assigned the TMD-2 and TMD-3 to be structurally similar to the TMD in lipid flippase MsbA (Chang, 2003) (a homologue of Multidrug Resistance ABC transporters, PDB

DMD #14241

entry:1pf4). The crystal structure of MsbA, solved at 3.8 Å resolution, consisted of a homodimer (chain A and B), where two of the TMDs were captured in a closed conformation. To build the 3D structures for TMD-2 and -3 of ABCC2, we took the TMD in chain A of 1pf4 as the template for TMD-2, and the TMD in chain B as the structural template for TMD-3. Due to the low sequence identity between ABCC2 (TMD-2 and -3) and 1pf4 (TMD), the alignments generated by the different fold recognition methods were quite different. As shown in Figure 1, the alignments from fold recognition methods are much more similar than the ones obtained with ClustalW. Interestingly, the alignments from FFAS and SAMT99 are highly consistent, although the algorithms for constructing the alignments were different. Therefore, in the present study we used this consensual alignment for the homology modeling of TMD-2 and -3 of ABCC2. After a minor manual optimization of this alignment by an additional prediction of TMHs, we built the 3D structure for TMD-2 and TMD-3 of ABCC2 by using the WhatIf software (Vriend, 1990). Furthermore, several small loops within the cavity formed by TMD-2 and -3 were built by using the Biopolymer module of the Sybyl modeling package (Tripos Inc). After the refinement of the side-chains, the addition of all hydrogen atoms, and energy minimization of the structure, the final 3D model of ABCC2 was generated (Figure 2).

The validation of the ABCC2 model built by fold recognition methods consisted of evaluating if it was able to recognize ABCC2 substrates and inhibitors. To reach this goal, a reference dataset of molecules consisting of 17 known ABCC1 and ABCC2 substrates and inhibitors was compiled (see Table 1). This dataset was designed after a careful inspection of the available literature using the SciFinder [37] searching interface to the Chemical Abstracts

DMD #14241

Database. During the search no specific ABCC2 substrates and inhibitors were found. Most of them interacted with both ABCC1 and ABCC2 but at different effective concentrations.

*Molecular dataset with quercetin glucuronides* - A second dataset, composed of quercetin-3-glucuronide, quercetin-3'-glucuronide, quercetin-4'-glucuronide and quercetin-7-glucuronide, was built. Each molecule was manually designed and minimized with the Sybyl molecular modeling package using the Tripos force field in order to optimize these structures. As ABCC2 is a major canalicular organic anion transporter, the anionic form of the compounds was also investigated.

*Virtual Screening of the reference database* - We used two well-known fixed protein-flexible ligand docking software packages, GOLD (Cambridge Crystallographic Data Center) and Glide (Schrödinger Inc.) to perform molecular docking calculations on the ABCC2 model. Firstly, a global docking calculation was carried out on the transporter with no *a priori* knowledge about the binding site location. This calculation was performed with the GOLD program as it permits the definition of a large binding site. In this step, the protein-binding site was defined as the whole transporter. For every molecule of the reference database, we used the software to generate one solution. Looking at the resulting conformations of the compounds, we focused on the known inhibitors. We identified the protein residues that make contact with the ABCC2 substrates and inhibitors. These residues form the potential binding site of the transporter: Lys<sup>329</sup>, Met<sup>440</sup>, Ser<sup>444</sup>, Gln<sup>447</sup>, Ile<sup>476</sup>, Ile<sup>479</sup>, Gln<sup>543</sup>, Cys<sup>544</sup>, Val<sup>546</sup>, Phe<sup>550</sup>, Thr<sup>553</sup>, Val<sup>557</sup>, Ser<sup>558</sup>, Phe<sup>562</sup>, Asn<sup>587</sup>, Ile<sup>588</sup>, Leu<sup>589</sup>, Arg<sup>591</sup>, Met<sup>595</sup>, Met<sup>598</sup>, Met<sup>599</sup>, Trp<sup>1144</sup>, Phe<sup>1149</sup>, Trp<sup>1254</sup>, Arg<sup>1257</sup>, Met<sup>1258</sup>, Glu<sup>1260</sup> (cf. Figure 1). A second virtual screening calculation of the reference database was performed on the binding site defined above. The docking calculations were carried out with the GOLD and Glide docking software. For each, the same



DMD #14241

binding site was used and thirty solutions were generated for each ligand. When considering the Glide's docking score (GlideScore) that estimates the binding affinity of the molecule to the protein, we have selected the first solution predicted for each ligand (see Table 1). According to these results, the top-ranked molecules are ABCC2 inhibitors.

*Interaction with ABCC2 in vitro-* Isolated membranes of ABCC2-expressing Sf9 insect cells were used to measure vanadate-sensitive ATPase activity during incubation with test compounds as previously described (Sarkadi et al., 1992; Bakos et al., 2000). The compounds were dissolved in 50 % methanol as a 15 mM stock solution and tested between 13.7 and 300  $\mu$ M. Maximum methanol concentration in the assay was 1%, and this had no effect on the assay. In activation studies, the capability of the compound to stimulate ATPase activity is determined, compared to the stimulatory effect of probenecid, a well-known ATPase activator, as control. The maximal efficacy of the test compounds is expressed on a 0-100% scale, where 100 % is defined as the activation observed in the presence of probenecid (1 mM). EC<sub>50</sub> is defined as the concentration of the test compound needed to reach 50 % of the maximal efficacy of the compound. In inhibition assays, the compounds are tested for their ability to reduce the stimulatory effect of the control compounds on the respective ABC transporter. At least two independent experiments were carried out. EC<sub>50</sub>, maximal efficacy and standard deviation were calculated.

*Caco-2 cell culture* - The cells were cultured in Dulbecco's Modified Eagle's Medium high glucose (4500 mg glucose/l) with 20% fetal bovine serum, 100 U/ml penicillin-streptomycin, 1% non essential amino acids, 1.25  $\mu$ g/ml fungizone and 50  $\mu$ g/ml gentamycin in 10% CO<sub>2</sub> at 37°C. Cells were used at passages 29 to 35. Caco-2 cells were seeded into six-well-plates at a

DMD #14241

density of  $1 \times 10^6$  cells per well, the medium was changed every two days and the experiments were carried out 20 d after reaching confluence (Delie and Rubas, 1997). Quercetin was dissolved in dimethyl sulfoxide and added to the medium so that the final concentration of dimethyl sulfoxide added to the medium was 0.1%. On the day of the experiment the cell culture medium was aspirated, the cells were washed with 2 ml phosphate-buffered saline per well and then incubated with 2 ml of cell culture medium (without phenol red) with the addition of appropriate test compounds or DMSO as a control. After incubation, the medium of each well was transferred into a 5 ml tube, immediately acidified with 20  $\mu$ l acetic acid (1 M) and aliquots of 50  $\mu$ l were placed on dry ice to freeze and stored at  $-80^\circ\text{C}$ . Samples were analyzed by HPLC as described above.

## Results

The ABCC2 3D model was generated *in silico* as described above. We then performed an evaluation of its ability to recognize molecules that are known substrates of this transporter and that were included in our reference dataset. Because the binding mode of the ligand was initially unknown, a consensual approach was applied to predict the conformation of the molecules upon binding to the protein. For each ligand, the 30 conformations predicted by *Glide* were compared to the ones predicted by *Gold*. An RMSD (Root Mean Square Deviation) value was calculated to compare the predicted solutions pair by pair. Generally, it is believed that two conformations with an RMSD value less than 2 Å were representative of the same binding mode. For every molecule, the solutions with the smallest RMSD values were retained. The results are presented in Table 1. Applying a cut-off of 2 Å for the RMSD, 5

## DMD #14241

molecules were selected. Four out of the five turned out to be ABCC2 inhibitors, and the remaining one was an ABCC2 substrate. When ranking the molecules according to the GlideScore values, the best scoring solutions were found to be the ABCC2 inhibitors. This implies that the ABCC2 binding site residues make more favorable interactions with these molecules than with other ones from the reference dataset, such as the known ABCC2 substrates. In particular, the strongest ABCC2 inhibitor according to these docking studies was the anionic form of MK-571. Some residues were identified to be in contact with all the inhibitors, such as Phe<sup>550</sup>, Thr<sup>553</sup>, Val<sup>557</sup>, Asn<sup>587</sup>, Ser<sup>558</sup>, Trp<sup>1144</sup>, and Phe<sup>1149</sup>.

The inhibitors, baicalin and glycyrrhizin, contain one and two glucuronide moieties, and form a hydrogen bond with the residues Arg<sup>1257</sup> and Glu<sup>1260</sup>. Based on the above validation of the ABCC2 transporter model, structure-based molecular docking experiments were performed in order to check the interaction with quercetin glucuronides. Using the same parameters applied in the validation step, the dataset containing the quercetin glucuronides (quercetin-3-*O*- $\beta$ -D-glucuronide, quercetin-3'-*O*- $\beta$ -D-glucuronide, quercetin-4'-*O*- $\beta$ -D-glucuronide and quercetin-7-*O*- $\beta$ -D-glucuronide) were screened against the transporter model. Glide results are displayed in Table 1. According to their GlideScore values, it appears that they interact in a weaker way with the transporter than known ABCC2 inhibitors such as MK-571.

We then tested the predictions from the *in silico* interactions in an *in vitro* assay. The ATPase assay monitors compound-induced activation of the transporter ATPase (Bakos et al, 2000). Good substrates activate the ATPase while inhibitors or slowly transported substrates can be detected by their inhibitory activity on the activated transporter. Therefore, the ATPase assay can be used to measure the interaction of ABCC2 with possible substrates or inhibitors

DMD #14241

(Table 2). Quercetin-7-*O*- $\beta$ -D-glucuronide activated ABCC2 ATPase more efficiently than the positive control probenecid (162.5% vs 100 %). This activation was *additive* with probenecid, since in the presence of this activator, maximal activity reached a plateau at around 250%. Quercetin-3-*O*- $\beta$ -D-glucuronide was least effective at activating ABCC2, with an activity of 46.5% of the control and the EC<sub>50</sub> at 100  $\mu$ M. Co-application with probenecid showed some cooperativity but it was only significant at higher concentrations. There was some inhibition by quercetin-3-*O*- $\beta$ -D-glucuronide below 30  $\mu$ M, and activation above that concentration. The activation was additive with probenecid. Quercetin-3'-*O*- $\beta$ -D-glucuronide alone activated ABCC2 with a similar EC<sub>50</sub>, but with activation only 50% of that of quercetin-7-*O*- $\beta$ -D-glucuronide; on co-application with probenecid, however, quercetin-3'-*O*- $\beta$ -D-glucuronide showed no sign of any cooperativity or additivity in an inhibition-type experimental setup. Quercetin-4'-*O*- $\beta$ -D-glucuronide elevated transporter specific ATPase activity by 48.5% with a low EC<sub>50</sub> value of 19  $\mu$ M. However, the efficacy of the activation was less than the maximal activation seen with either quercetin-7-*O*- $\beta$ -D-glucuronide or quercetin-3'-*O*- $\beta$ -D-glucuronide due to the bimodal nature of the activation curve. Activation was *additive* with probenecid, since, in the presence of this *bona fide* activator, maximal activity peaked at 172% (Table 2).

A correlation between the experimental (EC<sub>50</sub>) and *in silico* calculated (GlideScore) binding affinity values was calculated. The correlation was reasonably good given the limited number of substrates, with a correlation coefficient of 0.80, and implies that computational molecular docking methods might be used to estimate the binding energies of other molecules that interact with this protein.

To determine the effects of *in situ* location of the transporter on interactions, we measured the metabolism of quercetin. Quercetin enters cells probably by passive diffusion,

DMD #14241

and is then conjugated in Caco-2 cells to form the methylated, glucuronidated and/or sulfated conjugates. We propose that the glucuronides, and possibly other conjugates, are then effluxed by ABCC2 back into the medium. We tested the effect of the ABCC2 inhibitors, MK571 and cyclosporin A, on the efflux. In the presence of up to 0.5 mM MK571, there was no apparent toxicity since Caco2 cell viability was unaffected as measured using neutral red.

Figure 3 shows some example chromatograms of the cell culture medium after incubation with quercetin in the presence and absence of MK571. The latter appears as a large peak towards the end of the chromatogram. Using the information from the chromatograms, the rates of formation of conjugates were calculated (Figure 4). Formation of quercetin 3- and 7-*O*- $\beta$ -D-glucuronide, and of 3' and 4'-methyl quercetin, is not saturated since the amount produced doubles as the dose of quercetin was increased two-fold. Quercetin 3'- and 4'-*O*- $\beta$ -D-glucuronide conjugates are apparently saturated i.e. the same amount of product is observed at both substrate concentrations (Fig. 4a). In the presence of the ABCC2 inhibitor, MK571, the profile of excreted metabolites is dramatically changed (Fig. 4b). In particular, quercetin-3-*O*- $\beta$ -D-glucuronide and quercetin-7-*O*- $\beta$ -D-glucuronide formation is abolished at both substrate concentrations and formation of quercetin-3' and 4'-*O*- $\beta$ -D-glucuronides are substantially decreased, demonstrating that MK571 blocks the transport of these compounds. In contrast, the formation or transport of 3'- and 4'-methyl quercetin is unaffected or even increased in the presence of MK571 at the lower quercetin concentration. Quercetin sulfates were also products of Caco2 cell metabolism. The results represent one or more sulfates of unknown substitution position, but clearly these are important products of metabolism. The formation as measured by efflux into the cell culture medium is inhibited by MK571, which suggests that quercetin

DMD #14241

sulfate(s) is also a substrate for ABCC2. The results with cyclosporin A were qualitatively similar but less pronounced (results not shown).

DMD #14241

## Discussion

Several studies using a number of models have concluded that ABCC2 is an important efflux transporter for quercetin conjugates, and we have used these conjugates to understand the mechanism of ABCC2. Here, we have built the 3D structure of ABCC2 (mainly TMD-2 and -3) via homology modeling. After the building of a three-dimensional structure for the human ABCC2, the model was challenged by molecular docking experiments. Based on the above docking results, the ABCC2 model allowed discrimination of some ABCC2 inhibitors from some ABCC2 substrates. A virtual screening calculation using a large database of natural compounds could be envisaged to identify new ABCC2 inhibitors. There was a reasonable correlation between the experimental EC<sub>50</sub> values for quercetin glucuronides and the GlideScore value that estimates the binding energy, obtained from the virtual screening experiments. Quercetin-3-*O*- $\beta$ -D-glucuronide and quercetin-3'-*O*- $\beta$ -D-glucuronide were predicted to have the weakest interaction by *in silico* modeling, and this was supported experimentally by binding and competition assays on ABCC2 over-expressing baculovirus-infected Sf9 cells. Furthermore, in the intact Caco-2 cell metabolism experiment, MK571, an inhibitor of ABCC2, decreased the amount of all quercetin glucuronides effluxed into the cell culture medium. Any differences between results from the Caco-2 cells and the other methods is probably due to the complicating presence of other transporters and conjugating enzymes in the cells.

The ABCC2 transporter is expressed in Caco-2 cells (Gutmann et al., 1999) at physiological levels (Taipalensuu et al., 2001), and has been localized to the apical membrane of Caco-2 cells by immunofluorescence (Walgren et al., 2000). The presence of a glucuronide

DMD #14241

transporter is necessary for glucuronidation by UGT to be effective (Cummings et al., 2004). ABCC2 is also expressed in liver, kidney, enterocytes, placenta and blood-brain barrier, and its activity is inhibited by depletion of intracellular GSH (Dietrich et al., 2003). ABCC2 interacts with a broad range of compounds such as glucuronide conjugates of several molecules, including endogenous (leukotriene C<sub>4</sub>, glutathione, conjugated bile salts such as monoglucuronosyl and diglucuronosyl bilirubin) and exogenous (methotrexate, ochratoxin A, doxorubicin, cisplatin, S-glutathionyl ethacrynic acid) compounds (Payen et al., 2002). ABCC2 is regulated by three distinct nuclear receptor signaling pathways (Pregnane X Receptor, Farnesoid X-activated receptor, and constitutive androstane receptor) (Kast et al., 2002). Quercetin blocks As(III) up-regulation of ABCC2 mRNA in hepatocytes, possibly due to increased GSH, but not through effects on JNK phosphorylation (Vernhet et al., 2001). Quercetin or *tert*-butyl hydroquinone coordinately induced UGT1A6 and ABCC2 in Caco-2 cells, whereas dioxin only induced UGT1A6, but not ABCC2 (Bock et al., 2000). Other polyphenols may interact with ABCC2; robinetin and myricetin effectively inhibited ABCC2, and the presence of a B-ring pyrogallol group was important for inhibition by the aglycone. Importantly, ABCC2 displayed a higher selectivity for flavonoid inhibition than ABCC1 (van Zanden et al., 2005). MK571 inhibited efflux of quercetin conjugates from HepG2 cells after treatment with quercetin-7-*O*- $\beta$ -D-glucuronide and quercetin-3-*O*- $\beta$ -D-glucuronide, although the quercetin-4'-*O*- $\beta$ -D-glucuronide was not taken up into the cells (O'Leary et al., 2003). However, these experiments were very much dependent on the uptake of the conjugates by an OATP-like transporter. ABCC2 and ABCG2 (BCRP) are both involved in quercetin metabolism and disposition. ABCC2-knock out (*Bcrp1*<sup>-/-</sup>) mice showed similar absorption of



DMD #14241

quercetin to the wild type, probably due to the compensating action of ABCG2 (Sesink et al., 2005) in the ABCC2 knock-out mouse.

It has been shown that ABCC2 has at least two binding sites. Positive cooperativity between substrates, as well as substrates and non-substrates, is common (Bakos et al., 2000;Zelcer et al., 2003;Bodo et al., 2003), and MK571 potentiates the transport of estradiol-17  $\beta$ -glucuronide by ABCC2 (Glavinas et al (unpublished data)). All the quercetin conjugates activated the ABCC2 ATPase albeit with different potencies and efficacies. More interestingly, all but quercetin-3'-*O*- $\beta$ -D-glucuronide showed an ATPase activation that seemed to be additive with probenecid-induced ABCC2 activation. An allosteric activation cannot therefore be completely ruled out. However, based on the correlation of the concentration dependence of ATPase activation and co-activation, allosteric activation is unlikely.

In summary, we have shown that an *in silico* generated structure of ABCC2 shows reasonable agreement with the experimentally-determined binding of quercetin glucuronides. So far it has proven difficult to make reliable models for *in silico* prediction of ABCB1 (MDR1/Pgp) – substrate interactions. This work shows that transporters, possibly with stricter substrate specificities, such as ABCC2, are more amenable to model building.

DMD #14241

## Reference List

Bakos E, Evers R, Sinko E, Varadi A, Borst P, Sarkadi B (2000). Interactions of the human multidrug resistance proteins MRP1 and MRP2 with organic anions. *Mol Pharmacol* **57**:760-768.

Bock KW, Eckle T, Ouzzine M, Fournel-Gigleux S (2000). Coordinate Induction by Antioxidants of UDP-glucuronosyltransferase UGT1A6 and the Apical Conjugate Export Pump MRP2 (multidrug resistance protein 2) in Caco - 2 Cells. *Biochem Pharmacol* **59**:467-470.

Bodo A, Bakos E, Szeri F, Varadi A, Sarkadi B (2003). Differential modulation of the human liver conjugate transporters MRP2 and MRP3 by bile acids and organic anions. *J Biol Chem* **278**:23529-23537.

Campbell JD, Koike K, Moreau C, Sansom MS, Deeley RG, Cole SP (2004). Molecular modeling correctly predicts the functional importance of Phe594 in transmembrane helix 11 of the multidrug resistance protein, MRP1 (ABCC1). *J Biol Chem* **279**:463-468.

Chang G (2003). Structure of MsbA from *Vibrio cholera*: a multidrug resistance ABC transporter homolog in a closed conformation. *J Mol Biol* **330**:419-430.

Crespy V, Morand C, Manach C, Besson C, Demigne C, Remesy C (1999). Part of quercetin absorbed in the small intestine is conjugated and further secreted in the intestinal lumen. *Am J Physiol-Gastroint Liver Physiol* **40**:G120-G126.

DMD #14241

Crespy V, Nancoz N, Oliveira M, Hau J, Courtet-Compondu MC, Williamson G (2004).

Glucuronidation of the green tea catechins, (-)-epigallocatechin-3-gallate and (-)-epicatechin-3-gallate, by rat hepatic and intestinal microsomes. *Free Radic Res* **38**:1025-1031.

Cummings J, Zelcer N, Allen JD, Yao D, Boyd G, Maliepaard M *et al.* (2004).

Glucuronidation as a mechanism of intrinsic drug resistance in colon cancer cells: contribution of drug transport proteins. *Biochem Pharmacol* **67**:31-39.

Day AJ, Bao Y, Morgan MRA, Williamson G (2000). Conjugation position of quercetin glucuronides and effect on biological activity. *Free Rad Biol Med* **29**:1234-1243.

Day AJ, Mellon FA, Barron D, Sarrrazin G, Morgan MRA, Williamson G (2001). Human Metabolism of dietary flavonoids: identification of plasma metabolites of quercetin. *Free Rad Res* **212**:941-952.

Delie F, Rubas W (1997). A human colonic cell line sharing similarities with enterocytes as a model to examine oral absorption: Advantages and limitations of the CaCo-2 model. *Crit Rev Ther Drug Carrier Syst* **8**:305-330.

Dietrich CG, Geier A, Oude Elferink RP (2003). ABC of oral bioavailability: transporters as gatekeepers in the gut. *Gut* **52**:1788-1795.

Gee JM, DuPont MS, Day AJ, Plumb GW, Williamson G, Johnson IT (2000). Intestinal transport of quercetin glycosides in rats involves both deglycosylation and interaction with the hexose transport pathway. *J Nutr* **130**:2765-2771.

DMD #14241

Gerk PM, Vore M (2002). Regulation of expression of the multidrug resistance-associated protein 2 (MRP2) and its role in drug disposition. *J Pharmacol Exp Ther* **302**:407-415.

Gutmann H, Fricker G, Torok M, Michael S, Beglinger C, Drewe J (1999). Evidence for different ABC-transporters in Caco-2 cells modulating drug uptake. *Pharm Res* **16**:402-407.

Janisch KM, Williamson G, Needs P, Plumb GW (2004). Properties of quercetin conjugates: modulation of LDL oxidation and binding to human serum albumin. *Free Radic Res* **38**:877-884.

Jaroszewski L, Rychlewski L, Zhang B, Godzik A (1998). Fold prediction by a hierarchy of sequence, threading, and modeling methods. *Protein Sci* **7**:1431-1440.

Karplus K, Barrett C, Hughey R (1998). Hidden Markov models for detecting remote protein homologies. *Bioinformatics* **14**:846-856.

Kast HR, Goodwin B, Tarr PT, Jones SA, Anisfeld AM, Stoltz CM *et al.* (2002). Regulation of multidrug resistance-associated protein 2 (ABCC2) by the nuclear receptors pregnane X receptor, farnesoid X-activated receptor, and constitutive androstane receptor. *J Biol Chem* **277**:2908-2915.

Konig J, Nies AT, Cui YH, Leier I, Keppler D (1999). Conjugate export pumps of the multidrug resistance protein (MRP) family: localization, substrate specificity, and MRP2-mediated drug resistance. *Biochim Biophys Acta* **1461**:377-394.

DMD #14241

Morand C, Crespy V, Manach C, Besson C, Demigne C, Remesy C (1998). Plasma metabolites of quercetin and their antioxidant properties. *Amer J Physiol Regul Integr C* **44**:R212-R219.

Nagasaka Y, Nakamura K (1998). Modulation of the heat-induced activation of mitogen-activated protein (MAP) kinase by quercetin. *Biochem Pharmacol* **56**:1151-1155.

O'Leary KA, Day AJ, Needs PW, Mellon FA, O'Brien NM, Williamson G (2003). Metabolism of quercetin-7- and quercetin-3-glucuronides by an in vitro hepatic model: the role of human beta-glucuronidase, sulfotransferase, catechol-O-methyltransferase and multi-resistant protein 2 (MRP2) in flavonoid metabolism. *Biochem Pharmacol* **65**:479-491.

O'Leary KA, Day AJ, Needs PW, Sly WS, O'Brien NM, Williamson G (2001). Flavonoid glucuronides are substrates for human liver beta-glucuronidase. *FEBS Lett* **503**:103-106.

Pascual-Teresa S, Johnston KL, DuPont MS, O'Leary KA, Needs PW, Morgan LM *et al.* (2004). Quercetin Metabolites Downregulate Cyclooxygenase-2 Transcription in Human Lymphocytes Ex Vivo but Not In Vivo. *J Nutr* **134**:552-557.

Payen L, Sparfel A, Courtois L, Vernhet A, Guillouzo A, Fardel O (2002). The drug efflux pump MRP2: Regulation of expression in physiopathological situations and by endogenous and exogenous compounds. *Cell Biol Toxicol* **18**:221-233.

Petri N, Tannergren C, Holst B, Mellon FA, Bao Y, Plumb GW *et al.* (2003).

Absorption/Metabolism of sulforaphane and quercetin, and regulation of phase ii enzymes, in human jejunum in vivo. *Drug Metab Dispos* **31**:805-813.

DMD #14241

Pulaski L, Jedlitschky G, Leier I, Buchholz U, Keppler D (1996). Identification of the multidrug-resistance protein (MRP) as the glutathione-S-conjugate export pump of erythrocytes. *Eur J Biochem* **241**:644-648.

Sarkadi B, Price EM, Boucher RC, Germann UA, Scarborough GA (1992). Expression of the human multidrug resistance cDNA in insect cells generates a high activity drug-stimulated membrane ATPase. *J Biol Chem* **267**:4854-4858.

Sesink A, Arts I, de B, V, Breedveld P, Schellens J, Hollman P *et al.* (2005). Breast Cancer Resistance Protein (Bcrp1/Abcg2) limits net intestinal uptake of quercetin in rats by facilitating apical efflux of glucuronides. *Mol Pharmacol.* **67**:1999-2006.

Shi J, Blundell TL, Mizuguchi K (2001). FUGUE: sequence-structure homology recognition using environment-specific substitution tables and structure-dependent gap penalties. *J Mol Biol* **310**:243-257.

Spencer JPE, Rice-Evans C, Williams RJ (2003). Modulation of pro-survival Akt/protein kinase B and ERK1/2 signaling cascades by quercetin and its in vivo metabolites underlie their action on neuronal viability. *Journal of Biological Chemistry* **278**:34783-34793.

Taipalensuu J, Tornblom H, Lindberg G, Einarsson C, Sjoqvist F, Melhus H *et al.* (2001). Correlation of gene expression of ten drug efflux proteins of the ATP-binding cassette transporter family in normal human jejunum and in human intestinal epithelial Caco-2 cell monolayers. *J Pharmacol Exp Ther* **299**:164-170.

DMD #14241

Uda Y, Price KR, Williamson G, Rhodes MJC (1997). Induction of the anticarcinogenic marker enzyme, quinone reductase, in murine hepatoma cells *in vitro* by flavonoids. *Cancer Letters* **120**:213-216.

van Zanden JJ, Wortelboer HM, Bijlsma S, Punt A, Usta M, Bladeren PJ *et al.* (2005). Quantitative structure activity relationship studies on the flavonoid mediated inhibition of multidrug resistance proteins 1 and 2. *Biochem Pharmacol* **69**:699-708.

Vernhet L, Seite MP, Allain N, Guillouzo A, Fardel O (2001). Arsenic induces expression of the multidrug resistance-associated protein 2 (MRP2) gene in primary rat and human hepatocytes. *J Pharmacol Exp Ther* **298**:234-239.

Vriend G (1990). WHAT IF: a molecular modeling and drug design program. *J Mol Graph* **8**:52-56.

Walgren RA, Karnaky KJ, Jr., Lindenmayer GE, Walle T (2000). Efflux of dietary flavonoid quercetin 4'-beta-glucoside across human intestinal Caco-2 cell monolayers by apical multidrug resistance-associated protein-2. *J Pharmacol Exp Ther* **294**:830-836.

Wortelboer HM, Usta M, van der Velde AE, Boersma MG, Spenkelink B, van Zanden JJ *et al.* (2003). Interplay between MRP inhibition and metabolism of MRP inhibitors: the case of curcumin. *Chem Res Toxicol* **16**:1642-1651.

Zelcer N, Reid G, Wielinga P, Kuil A, van dH, I, Schuetz JD *et al.* (2003). Steroid and bile acid conjugates are substrates of human multidrug-resistance protein (MRP) 4 (ATP-binding cassette C4). *Biochem J* **371**:361-367.

DMD #14241

Footnote: \*Solvo Biotechnology has been supported by grants FP6-2004-LIFESCIHEALTH-5; Proposal No 018961, FP6-2004-LIFESCIHEALTH-5; Proposal No 518246, FP6, Network of Excellence (BioSim) 005137, and Hungarian grants GVOP 3.1.1 – 2004-05-0506/3.0, GVOP 3.1.1 – 2004-05-0440/3.0, GVOP Munka - 00034/2003, NKFP 1/A-041/04, RET,- Debrecen, OTKA T 043141. PN and PAK are supported by the Biotechnology and Biological Sciences Research Council, UK. GW, IA, LM, ZZ, MBS, VC, DB and MG are, or were, employees of Nestlé SA, Switzerland.

Reprints to: Gary Williamson, Nestlé Research Center, Vers Chez Les Blanc, 1000 Lausanne 26, Switzerland, Tel. +41217858546; Fax. +41217858544;

E-mail: [gary.williamson@rdls.nestle.com](mailto:gary.williamson@rdls.nestle.com)



DMD #14241

## FIGURE LEGENDS

Fig. 1: Comparison of the sequence alignments based on different methods.

(a) The sequence alignment between TMD-2 and 1pf4 (Chain: A)

(b) The sequence alignment between TMD-3 and 1pf4 (Chain: B)

<sup>a</sup>.The prediction of Trans-membrane Helices (TMHs) was taken from the annotation in the Swissprot database.

<sup>b</sup> For comparison, the alignment from classical sequence alignment method (i.e. ClustalW) was also displayed.

mrp2tmd2 and mrp2tmd3 refer to the trans-membrane domains (TMD) 2 and 3 of MRP2, respectively. 1pf4 is the template lipid flippase protein, samt99, ffas and fugue denote the sequence alignments obtained by different fold recognition algorithms.

The residues in the proposed active site are in bold.

Fig. 2: Structure of the ABCC2 transporter generated *in silico* as described in the experimental section.

Fig. 3: HPLC chromatogram of quercetin metabolites. The top chromatogram shows the elution of a mixture of standards (A, B, C, D, F, G, H, and I). After incubation of quercetin with Caco-2 cells for 8 h, in the presence (middle chromatogram) and absence (lower chromatogram) of MK571, quercetin conjugates can be clearly seen. Peak E was identified as sulfate(s) since the peak disappeared after sulfatase treatment. Other peaks are indicated as

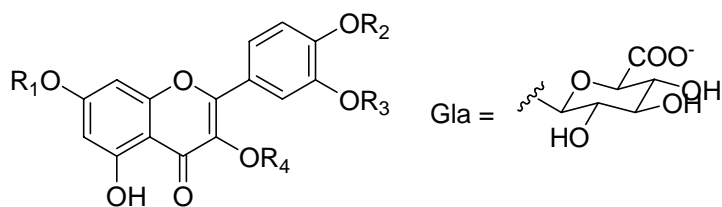
DMD #14241

follows: A= quercetin-3-*O*- $\beta$ -D-glucuronide; B= quercetin-7-*O*- $\beta$ -D-glucuronide;  
C=quercetin-4'-*O*- $\beta$ -D-glucuronide; D=quercetin-3'-*O*- $\beta$ -D-glucuronide; F= quercetin;  
G=apigenin (internal standard); H= 3'-methyl-quercetin; I= 4'-methyl-quercetin; J=MK571.

Fig. 4: Release of quercetin into Caco-2 cell culture medium in the (a) absence and (b) presence of MK571. The concentration of conjugate at 4 h was used to estimate a rate of the conjugation reaction. Initial quercetin concentration was 20  $\mu$ M (unfilled bars) or 40  $\mu$ M (filled bars). The bar for sulfate is unassigned quercetin sulfate conjugates. The error bars indicate standard deviation (n = 3). 3glcA = quercetin-3-*O*- $\beta$ -D-glucuronide, 7glcA = quercetin-7-*O*- $\beta$ -D-glucuronide, 3'glcA = quercetin-3'-*O*- $\beta$ -D-glucuronide, 4'glcA = quercetin-4'-*O*- $\beta$ -D-glucuronide, SO4 = mixed quercetin sulfates, 3'Me = 3'-methyl quercetin, 4'Me = 4'-methyl quercetin. At 4 h, free quercetin concentration in the medium was 2 and 9  $\mu$ M after an initial concentration of 20 and 40  $\mu$ M respectively.

DMD #14241

Scheme 1. Structure of quercetin conjugates (anionic form)



$R_1 = R_2 = R_3 = H, R_4 = \text{Gla}$ : Quercetin 3-*O*- $\beta$ -D-glucuronide

$R_1 = \text{Gla}, R_2 = R_3 = R_4 = H$ : Quercetin 7-*O*- $\beta$ -D-glucuronide

$R_1 = R_2 = R_4 = H, R_3 = \text{Gla}$ : Quercetin 3'-*O*- $\beta$ -D-glucuronide

$R_1 = R_3 = R_4 = H, R_2 = \text{Gla}$ : Quercetin 4'-*O*- $\beta$ -D-glucuronide

DMD #14241

Table 1. Virtual screening results for the reference and the quercetin glucuronide datasets

Name	Anionic Form	Activity <sup>a</sup>	GlideScore <sup>b</sup>	RMSD <sup>c</sup>
MK-571	Yes	Inhibitor	-11.11	1.73
Glibenclamide	No	Inhibitor	-8.93	1.86
SDZ-PSC 833	No	Inhibitor	-8.90	2.38
MK-571	No	Inhibitor	-8.85	2.96
Verapamil	No	Inhibitor	-8.82	1.84
Quercetin-4'- <i>O</i> - $\beta$ -D-glucuronide	Yes	Substrate	-8.6	1.75
Glycyrrhizin	No	Inhibitor	-8.59	2.10
Baicalin	No	Inhibitor	-8.59	2.19
Quercetin-7- <i>O</i> - $\beta$ -D-glucuronide	Yes	Substrate	-8.52	1.37
Baicalin	Yes	Inhibitor	-8.41	1.03
Taxol	No	Inhibitor	-8.34	2.61
Quercetin-3'- <i>O</i> - $\beta$ -D-glucuronide	Yes	Substrate	-8.28	1.59
Quercetin-3- <i>O</i> - $\beta$ -D-glucuronide	Yes	Substrate	-7.66	1.34
Grepafloxacin	Yes	Substrate	-7.62	1.30
Ampicillin	No	Substrate	-7.39	2.51
Ampicillin	Yes	Substrate	-6.86	2.11
Quercetin	No	Substrate	-6.82	2.05
Grepafloxacin	No	Substrate	-6.74	2.19

<sup>a</sup> Activity towards ABCC2 according to literature. <sup>b</sup> Glide energy units.

<sup>c</sup> RMSD between the energetically-preferred (“best”) GOLD and Glide solution for each ligand.

DMD #14241

Table 2: Interaction of quercetin glucuronides with ABCC2 over-expressed baculovirus-infected Sf9 cell membranes.

	ATPase activation <sup>a</sup>		ATPase inhibition <sup>a, b</sup>	
	EC <sub>50</sub> (μM)	Maximum efficacy (%)	EC <sub>50</sub> (μM)	Maximum efficacy (%)
Quercetin-7- <i>O</i> -β-D-glucuronide	61 +/- 1.4	162.5 +/- 53.0	55 +/- 9.9	163 +/- 89.1
Quercetin-3- <i>O</i> -β-D-glucuronide	100 +/- 1.4	46.5 +/- 6.4	95 +/- 7.1	27 +/- 9.9
Quercetin-3'- <i>O</i> -β-D-glucuronide	50 +/- 22.6	85 +/- 56.6	-	-
Quercetin-4'- <i>O</i> -β-D-glucuronide	19 +/- 1.4	48.5 +/- 2.1	6 +/- 1.4	72 +/- 21.2

<sup>a</sup>Vanadate sensitive ATPase activity in the absence of probenecid (basal activity) was 9,2 +/- 2,3 nmol Pi/mg protein/min. In the presence of 1 mM probenecid (activated ATPase) the vanadate sensitive ATPase activity was 18,8 +/- 2,0 nmol Pi/mg protein/min.

<sup>b</sup>In inhibition experiments the test compounds showed an ATPase activation that was additive with probenecid

Fig 1a

mrp2tmd2	KSGTKKDVPKSWLMKALFKTFYMVLLKSFLKLVNDIFTFVSPQLLKLKLLISFASDRDITYL
TMH <sup>a</sup>	-----h h h h h h h h h h h h h h h h h h h-----
samt99	.....WQTFKRLWTYIRLYKAGLVVSTIALVINAAADTYMISLLKPLLDEGF.GNAES
ffas	LHSDES <sup>b</sup> WQTFKRLWTYIRLYKAGLVVSTIALVINAAADTYMISLLKPLLDEGF.GNAES
fugue	.....WQTFKRLWTYIRLYKAGLVVSTIALVINAAADTYMISLLKPLLDEGF <sup>b</sup> GNAESN
clustalw <sup>b</sup>	.MSLHSDES <sup>b</sup> WQTFKRLWTYIRLYKAGLVVSTIALVINAAADTYMISLLKPLLDEGF <sup>b</sup> GNA
mrp2tmd2	WIGYLCAILLFTAALIQSFC <sup>b</sup> LQCYFQLCFKLGVKVRTAIMASVYKKAL <sup>b</sup> TLN <sup>b</sup> LARKEYTV
TMH	---h h h h h h h h h h h h h h h h h h h-----
samt99	NFLRILPFMILGLMFVRGLSGFASSYCLSWVSGNVVMQMRRLFNHFMHPVRRFFDQEST
ffas	NFLRILPFMILGLMFVRGLSGFASSYCLSWVSGNVVMQMRRLFNHFMHPVRRFFDQEST
fugue	FLRIL.PFMILGLMFVRGLSGFASSYCLSWVSGNVVMQMRRLFNHFMHPVRRFFDQEST
clustalw	ESNFLRILPFMILGLMFVRGLSGFASSYCLSWVSVVMQMRRLFNHFMHPVRRFFDQEST
mrp2tmd2	GETVNLMSVDAQKLM <sup>b</sup> DVTNFM <sup>b</sup> MLWS <sup>b</sup> SVLQIVLSIFFLWRELGPSVL <sup>b</sup> AGVGMVLVIPIN
TMH	-----h h h h h h h h h h h h h h h h h h h-----h h h h h h h h h h h h h h h
samt99	GGLLSRITYDSEQVAGATSRLVSIVREGASIIIGLLTLMFWNSWQLSLVLIVVAPVVAFAI
ffas	GGLLSRITYDSEQVAGATSALVSIVREGASIIIGLLTLMFWNSWQLSLVLIVVAPVVAFAI
fugue	GGLLSRITYDSEQVAGATSRLVSIVEGASIIIGLLTLMFWNSWQLSLVLIVVAPVVAFAI
clustalw	GGLLSRITYDSEQVAGATSLVSIV REGASIIIGLLTLMFWNSWQLSLVLIVVAPVVAFAI
mrp2tmd2	AILSTKSKTIQVKNMKNKDKRLKIMNEILSGIKILKYFAWEPSFRDQVQNL <sup>b</sup> RKKELKNLL
TMH	hhh-----
samt99	SFVSKRFRKISRNMQTAMGH.....RQQT <sup>b</sup> M
ffas	SFVSKRFRKISRNMQTAMGHVTS <sup>b</sup> SAEQMLKGHKVVLSYGGQEVERKRFDKVSN <sup>b</sup> SMRQQT <sup>b</sup> M
fugue	SFVSKRFRKISRNMQTA.....M <sup>b</sup> GHRQQT <sup>b</sup> MKL <sup>b</sup> VSAQS <sup>b</sup> IADPVIQMIASLALFAVLFLA
clustal	SFVSKRFRKISRNMQTAMGHVTS <sup>b</sup> SAEQMLKGHKVVLSYGGQEVERKRFDKVSN <sup>b</sup> SMRQQT <sup>b</sup> M
mrp2tmd2	AFS <sup>b</sup> QLQCVVIFVFQ <sup>b</sup> LTPVLVSVVTF <sup>b</sup> SVYVLVDSNNILDAQKAFTSITL <sup>b</sup> FNILFRPLSMLP
TMH	-----h h h h h h h h h h h h h h h h h h h-----h h h h h h h h h h h h h h h
samt99	KL <sup>b</sup> VSAQSIADPVIQMIASLALFAVLFLASVDSIRAELTPGTFTVVFSAMFGLMRPLKALT
ffas	KL <sup>b</sup> VSAQSIADPVIQMIASLALFAVLFLASVDSIRAELTPGTFTVVFSAMFGLMRPLKALT
fugue	SVDSI.....RAELTPGTFTVVFSAMFGLMRPLKALT
clustalw	KL <sup>b</sup> VSAQSIADPVIQMIASLALFAVLFLASVDSIRAELTPGTFTVVFSAMFGLMRPLKALT
mrp2tmd2	MMISS
TMH	hhhhh
samt99	SVTSE
ffas	SVTSE
fugue	SVTSE
clustalw	SVTSE

Fig 1b

```
mrp2tmd3      TGKVKFSIYLEYLQAIGLFSIFFIILAFVMNSVAFIGSNLWLSAWTSDSKI FNSTDYPAS
TMH           -----hhhhhhhhhhhhhhhhhhhh-----
samt99       .....LWTYIRLYKA.GLVVSTIALVINAAADTYMISLLKPLLDEGFGNAESNF...
ffas         .....FKRLWTYIRLYKA.GLVVSTIALVINAAADTYMISLLKPLLDEGFGNAESN....
fugue        .....WQTFKRLWTYIRLYK..AGLVVSTIALVINAAADTYMISLLKPLLDEGFGNAESN
clusatlw     MSLHSDESNEWQTFKRLWTYIRLYKAGLVVSTIALVINAAADTYMISLLKPLLDEGFGNAE

mrp2tmd3      QRDMRVGVYGALGLAQGIFVFI AHFWSAFGFVHASNILHKQLLNNILRAPMRFDDTTPTG
TMH           -----hhhhhhhhhhhhhhhhhhhh-----
samt99       .LRILPFMILGLMFVRGLSGFASSYCLSWVSGNVVMQMRRLFNHFHMPVRRFFDQESTG
ffas         FLRILPFMILGLMFVRGLSGFASSYCLSWVSGNVVMQMRRLFNHFHMPVRRFFDQESTG
clusatlw     SNFLRILPFMILGFVRGLSGFASSYCLSWVSGNVVMQMRRLFNHFHMPVRRFFDQESTG

mrp2tmd3      RIVNRFAGDISTVDDTLPQSLRSWITCFLGIISTLVMICMATPVFTIIVIPLGIIYVSQ
TMH           -----hhhhhhhhhhhhhhhhhhhh-----hhhhhhhhhhhhhhhhhhhh
samt99       GLLSRITYDSEQVAGATSRALVSIVREGASIIIGLLTLMFWNSWQLSLVLI VVAPVVAFAI
ffas         GLLSRITYDSEQVAGATSRALVSIVREGASIIIGLLTLMFWNSWQLSLVLI VVAPVVAFAI
fugue        GLLSRITYDSEQVAGATSRALVSIVREGASIIIGLLTLMFWNSWQLSLVLI VVAPVVAFAI
clusatlw     GLLSRITYDSEQVAGATSRALVSIVREGASIIIGLLTLMFWNSWQLSLVLI VVAPVVAFAI

mrp2tmd3      MFYVSTSRQLRRLDSVTRSPIYSHFSETVSGLPVIRAFEHQQRFLKHNEVRIDTNQKCVF
TMH           h-----
samt99       SFVSKRFRKISRNMQTAMGH.....RQOTM
ffas         SFVSKRFRKISRNMQTAMGHVTSSAEQMLKGHKVVL SYGGQEVERKRFDKVSNSMRQOTM
fugue        SFVSKRFRKISRNMQTA.....MGHRQOTM KLVSAQSIADPVIQMIASL.....
clusatlw     SFVSKRFRKISRNMQTAMGHVTSSAEQMLKGHKVVL SYGGQEVERKRFDKVSNSMRQOTM

mrp2tmd3      SWITSNRWLAIRLELVGNLTVFFSALMMVIYRDTLSGDTVGFVLSNALNITQTLNWLVRM
TMH           -----hhhhhhhhhhhhhhhhhhhh-----hhhhhhhhhhhhhhhhhhhh-----
samt99       KLVSAQSIADPVIQMIASL.FVLFLASVDSIRAELTPGTFTVVFSAMFGLMRPLKAL...
ffas         KLVSAQSIADPVIQMIALFAVLFLASVDSIRAELTPGTFTVV.FSAMFGLMRPLKALTSV
fugue        .....ALFAVLFLASVDSIRAELTPGTFTVVFSAMFGLMRPLKALTSV
clusatlw     KLVSAQSIADPVIQMIASLALFAVLFLASVDRAELTPGTFTVVFSAMFGLMRPLKALTSV

mrp2tmd3      TSEIETNIVA
TMH           -----
pdbblast     TSEFQRGMAA
samt99       .....
ffas         TSEFQRGMAA
fugue        TSEFQRGMAA
clusatlw     TSE.....
```

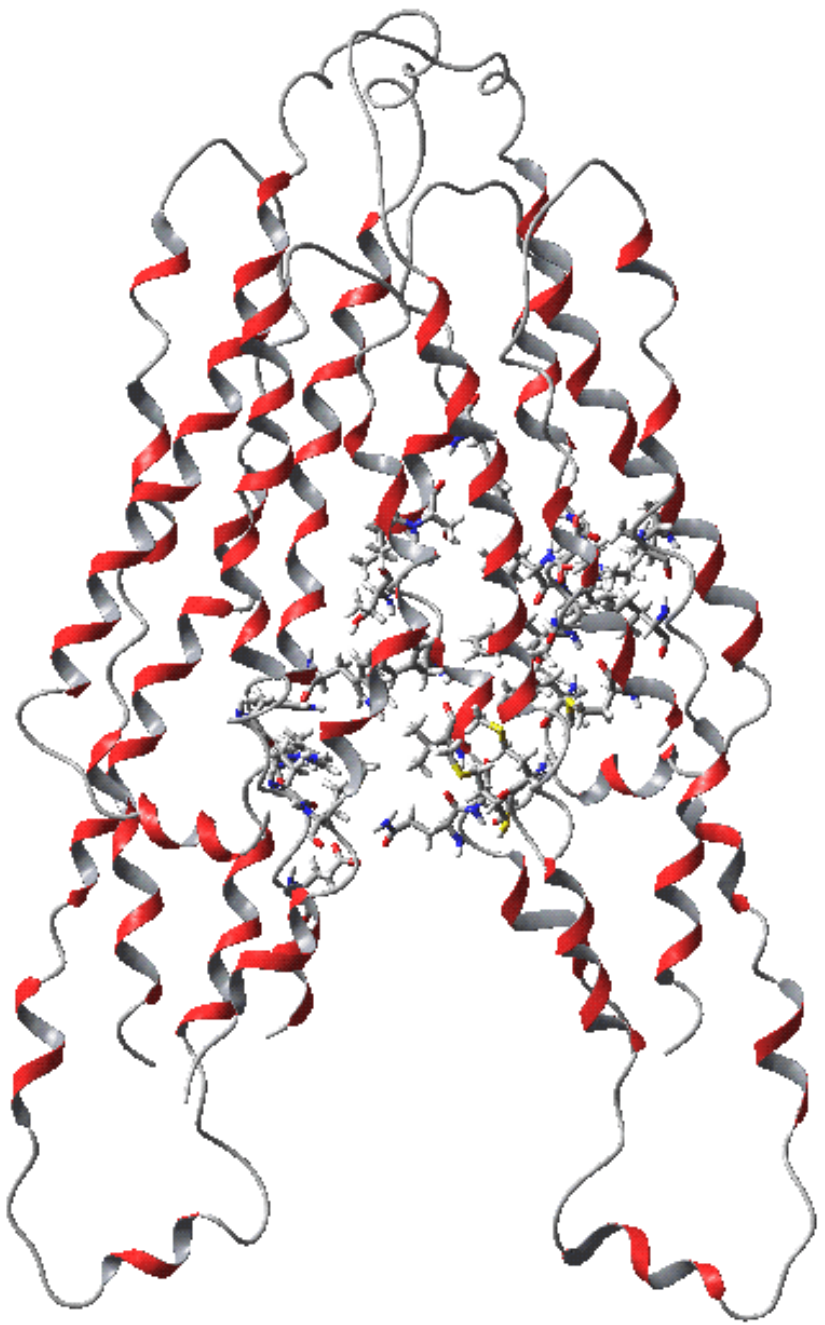


Fig 2



Fig 3

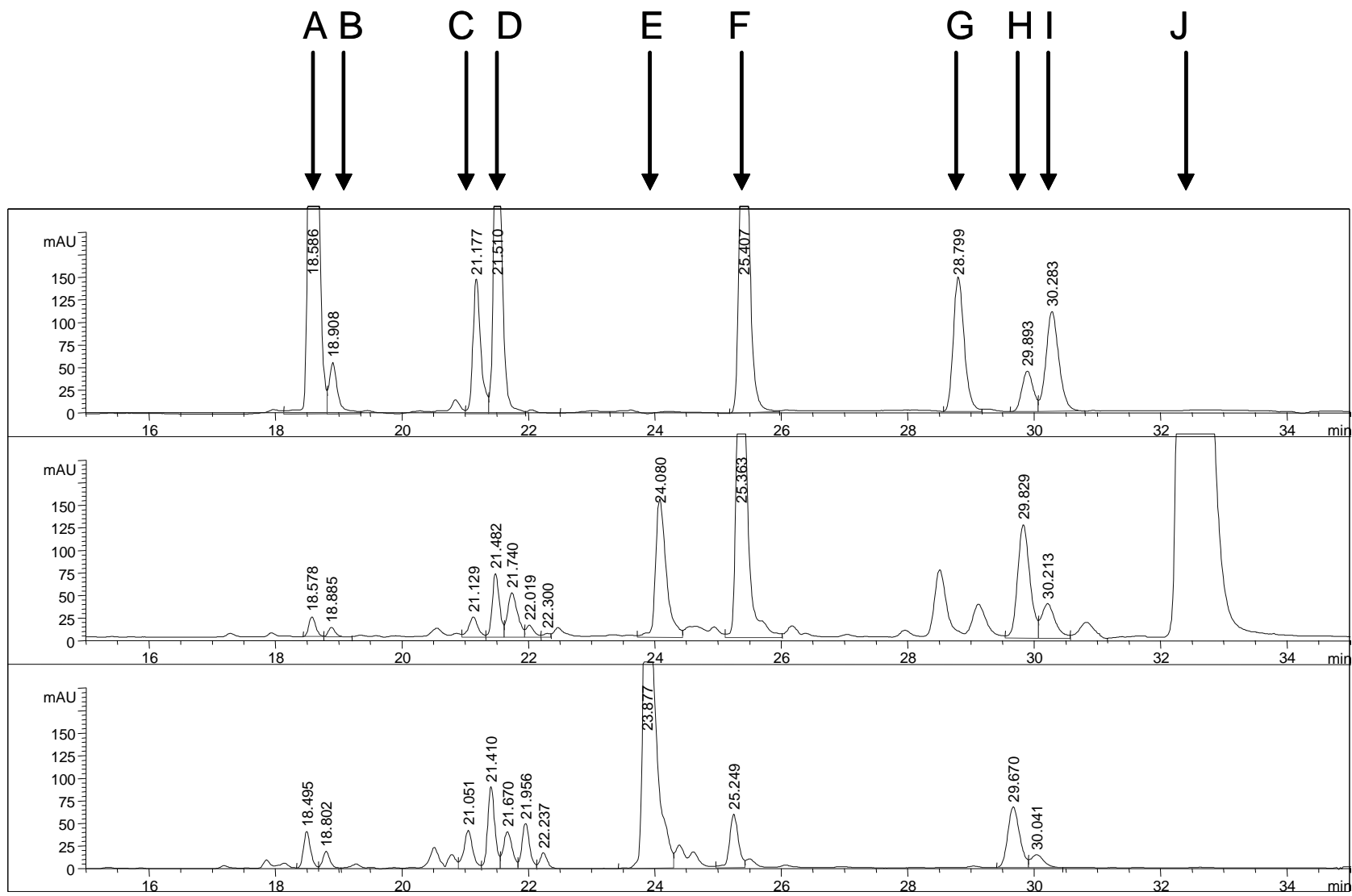


Fig 4a

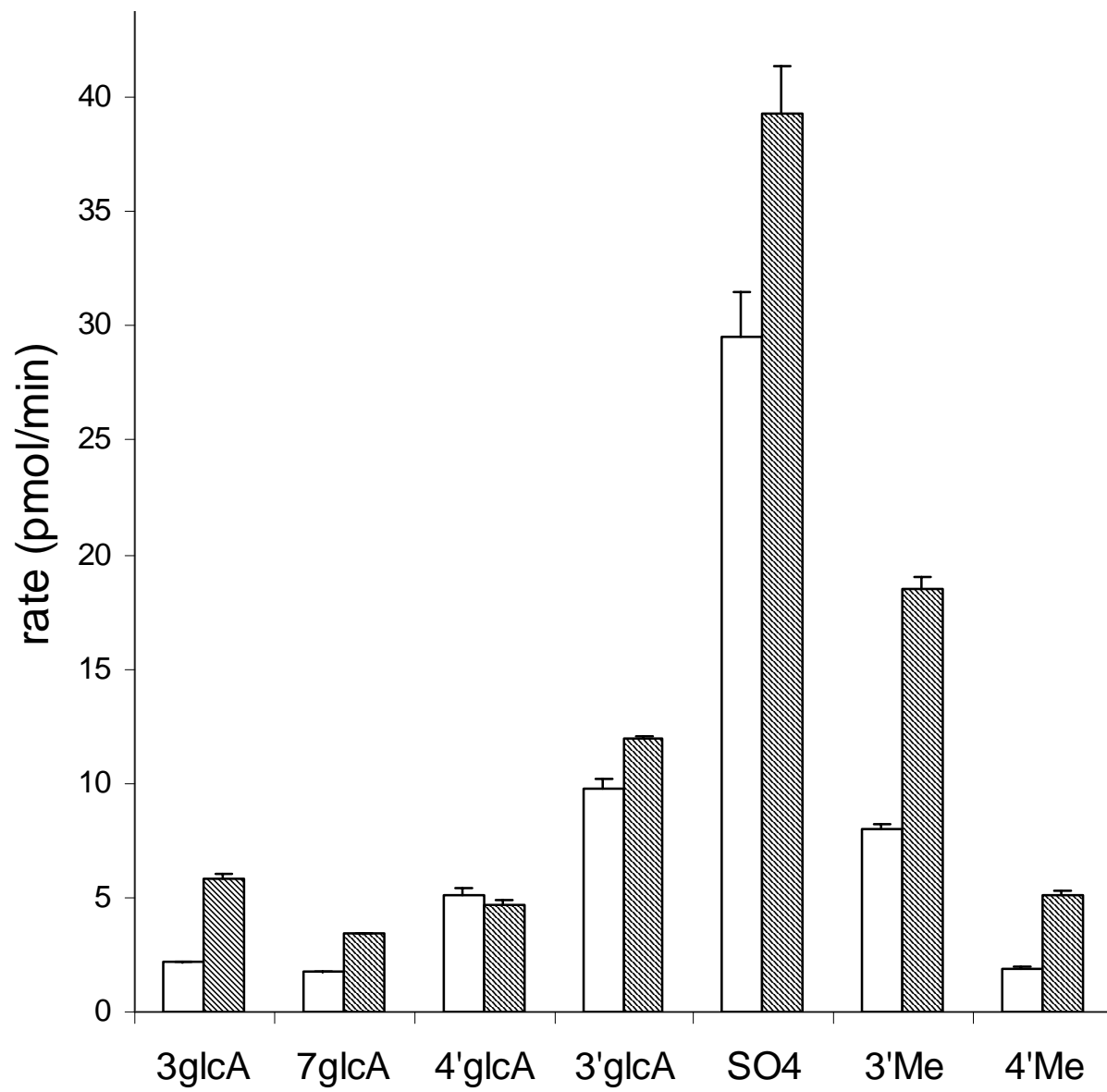


Fig 4b

